Response to reviewer2

Summary

The authors introduce a novel three-dimensional analytical framework to identify vertical teleconnection patterns in the Northern Hemispheric summer. By applying the teleconnection method to the meridional and zonal vertical stream functions derived from the three-pattern decomposition of global atmospheric circulation (3P-DGAC), the authors identify 14 distinct teleconnection patterns. They demonstrate that these patterns can effectively reconstruct summer surface air temperature and large-scale circulation anomalies, offering a new perspective on low-frequency variability. The framework is innovative and the results are scientifically intriguing, particularly the reconstruction skill for extreme heat years. However, the manuscript currently lacks a solid physical explanation for the proposed patterns, specifically regarding their dynamical origins and their relationship to established teleconnections. To ensure the robustness and physical relevance of these new indices, a revision is necessary.

Response:

We thank the reviewer for the constructive assessment of our work. We fully agree that a solid physical interpretation of the identified patterns, particularly regarding their dynamical origins and their relationship to established teleconnections, is essential. Following the reviewer's suggestions, we have added a Rossby wave activity flux analysis and a dedicated discussion on the physical drivers of the vertical circulation cells. We have also clarified the correspondence between our patterns and known teleconnections. Our detailed responses to each specific comment are provided below.

Specific Comments

1, The manuscript identifies 14 new teleconnection patterns based on statistical correlation, but it provides limited physical justification for their existence and maintenance. To demonstrate that these patterns are physically consistent with large-scale dynamics rather than merely statistical constructs, I recommend adding a Rossby wave activity flux analysis. This analysis would help visualize the propagation of wave energy associated with these vertical patterns, confirming whether they behave as true dynamical modes.

Response:

We thank the reviewer for this suggestion. Following the recommendation, we have computed the horizontal wave activity flux (Takaya and Nakamura, 2001) at 200 hPa and superimposed the vectors onto the regressed geopotential height anomalies in Figure 2. For the HCST pattern, the WAF vectors trace eastward energy propagation along the Asian subtropical jet, consistent with the behavior of the Silk Road Pattern. For the HSK pattern, the WAF vectors indicate energy propagation along the polar front jet from the British Isles toward the Kara Sea, consistent with the British–Baikal Corridor. The WAF analysis further confirms eastward energy dispersion along the mid-latitude waveguide for the HUB pattern, and coherent energy propagation pathways for the zonal patterns as well. These results confirm that the identified vertical circulation teleconnections are associated with coherent Rossby wave energy propagation, supporting their physical consistency with large-scale dynamics rather than being mere statistical constructs. We have revised Section 3.2 accordingly to include a discussion of the wave activity flux results (see lines 198–232).

Lines 198-232:

To capture the horizontal circulation signatures associated with these vertical teleconnections, the 200-hPa geopotential height (GHT) anomalies are regressed onto the respective vertical circulation indices with horizontal wave activity fluxes superimposed to diagnose the propagation of quasi-stationary Rossby wave energy

(Fig. 2). The resultant horizontal regression patterns corresponding to the 14 vertical teleconnections are designated as the HCP-series (HCP standing for "horizontal pattern"), as shown in Fig. 2.

Certain horizontal circulation patterns associated with the meridional vertical teleconnections (HCP-H series) manifest classical wave train signatures across the NH (Fig. 2). For instance, the HCP-HCB exhibits a zonal wave train spanning from the northeastern Pacific to the western Atlantic (Fig. 2b). The HCP-HCST displays a mid-latitude Eurasian wave train with anomaly centers over Eastern Europe, Western Asia, and Central Asia (Fig. 2c), which is structurally consistent with the Silk Road Pattern (SRP) (r = 0.89, p < 0.01; Fig. S3). The corresponding WAF vectors for HCST clearly trace eastward energy propagation along the Asian subtropical jet, confirming the wave-train nature of this teleconnection. The four-center structure of the HCP-HSK, extending from Britain to Lake Baikal (Fig. 2d), closely mirrors the British-Baikal Corridor (BBC) pattern (r = -0.77, p < 0.01; Fig. S4) , with WAF vectors indicating energy propagation along the polar front jet from the British Isles toward the Kara Sea. The HCP-HUB exhibits positive anomalies over the British Isles and northern Siberia contrasting with negative anomalies over western Russia (Fig. 2g), resembling the British-Okhotsk Corridor pattern (r = 0.74, p < 0.01; Fig. S5) The WAF analysis further confirms eastward energy dispersion along the mid-latitude waveguide for these patterns. Similarly, the horizontal circulation patterns linked to the seven zonal vertical teleconnections (the HCP-W series) demonstrate distinctive regional signatures. The HCP-WMCS exhibits a meridional dipole spanning from Greenland to Siberia (Fig. 2i), whereas the HCP-WWSJ shows a tripole structure across Greenland, Europe, and Siberia (Fig. 2j). Notably, the North Atlantic dipole pattern exhibited by the HCP-WGA (Fig. 2k) aligns closely with the summer North Atlantic Oscillation (NAO) pattern (Greatbatch and Rong 2006) Wave activity flux vectors for these zonal patterns consistently indicate coherent energy propagation pathways connecting the identified anomaly centers, further supporting their interpretation as genuine dynamical modes.

The analysis demonstrates that the horizontal patterns associated with these vertical teleconnections encompass many of the well-documented NH low-frequency modes (e.g., SRP, BBC, summer NAO). This consistency suggests that the proposed vertical circulation framework effectively captures key low-frequency variability patterns in the NH summer circulation. Hence, it serves as a robust approach for identifying essential atmospheric circulation characteristics. The WAF analysis confirms that these patterns are associated with coherent Rossby wave energy propagation, supporting their physical consistency with large-scale dynamics rather than being mere statistical constructs. Furthermore, this approach identifies several patterns not heavily emphasized in previous conventional analyses (e.g., HCP-WMCS, HCP-WGA, HCP-WOM), potentially offering new insights into the atmospheric dynamics linked to extreme weather events. Additionally, this framework supports the utility of 3P-DGAC stream functions for teleconnection analysis and enables the systematic comparison of previously identified modes within a unified three-dimensional perspective.

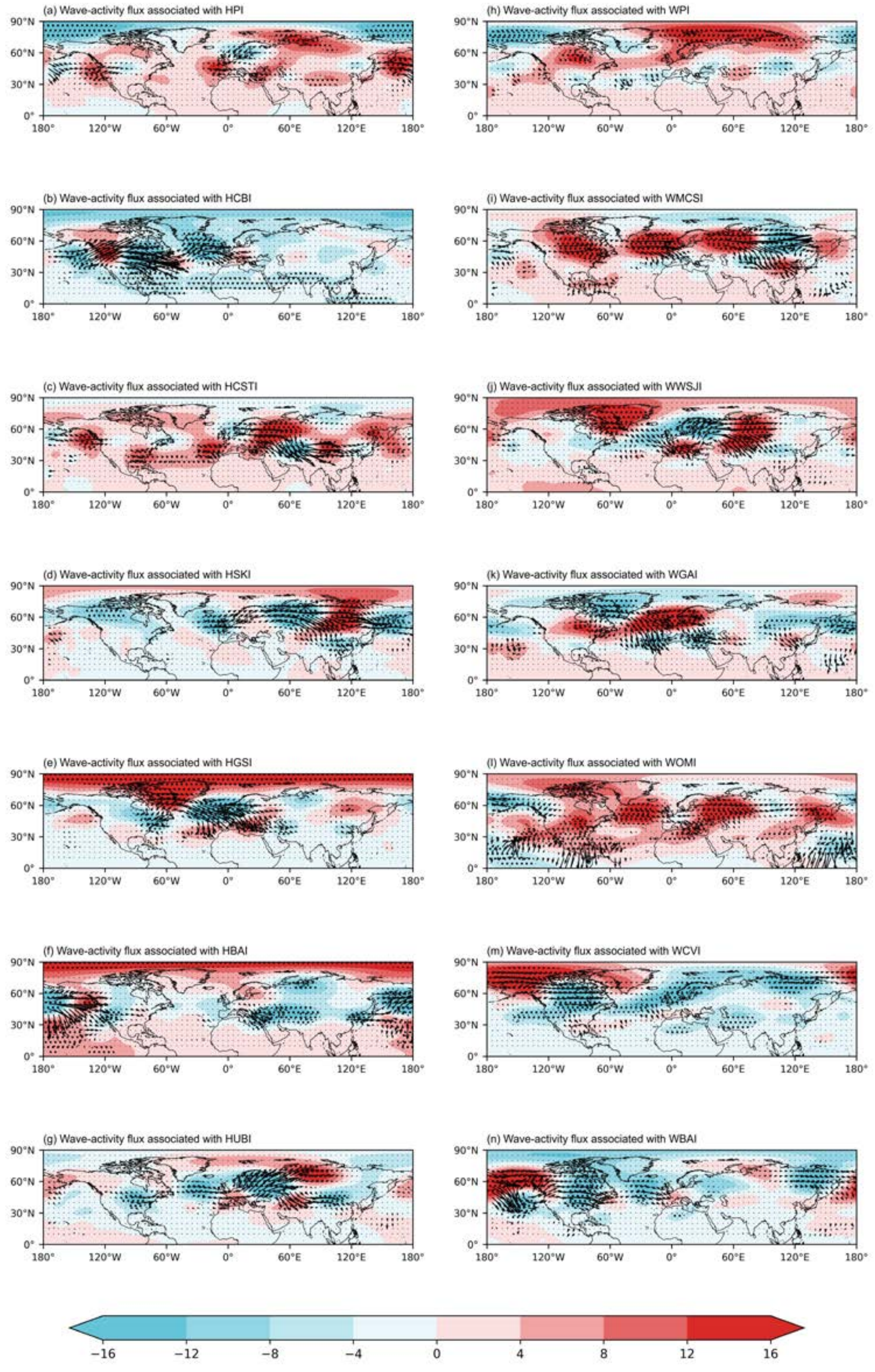

Figure 2. Regressed summer 200-hPa geopotential height anomalies (shading, units: gpm) onto the 14 teleconnection indices for the period 1979–2022, with horizontal wave activity fluxes (vectors, units: $m^2\ s^{-2}$) superimposed. (a)–(g) H-based patterns: (a) HPI, (b) HCBI, (c) HCSTI, (d) HSKI, (e) HGSI, (f) HBAI, (g) HUBI. (h)–(n) W-based patterns: (h) WPI, (i) WMCSI, (j) WWSJI, (k) WGAI, (l) WOMI, (m) WCVI, (n) WBAI. Vectors indicate the propagation direction of quasi-stationary Rossby wave energy; only vectors significant at the 95% confidence level are shown. Dotted areas indicate geopotential height anomalies significant at the 95% confidence level. Data are detrended prior to analysis.

2, The identification of vertical circulation cells is a key contribution of this work, but the physical drivers remain unclear. The manuscript should at least discuss the possible physical processes maintaining these vertical cells. Are they driven by diabatic heating, orographic forcing or land-atmosphere interactions? A brief dynamical interpretation would significantly strengthen the proposed framework.

Response:

We thank the reviewer for this important suggestion. We agree that a brief discussion of the physical drivers of the identified vertical circulation cells would strengthen the manuscript. Accordingly, we have added a new paragraph in the Discussion section to address this issue (see lines 401–418).

Lines 401–418:

The formation and evolution of the identified vertical circulations are closely linked to atmospheric dynamical processes and thermodynamic feedbacks, primarily governed by the atmospheric temperature anomaly gradient (ATAG) and the associated evolution of atmospheric baroclinicity. From a three-dimensional dynamical perspective, the development of large-scale three-dimensional circulations is fundamentally tied to the baroclinic structure characterized by horizontal temperature gradients. External forcings, including diabatic heating, air-sea interactions, and orographic forcing, can generate and modulate horizontal temperature gradients and the associated atmospheric baroclinicity by altering the spatially non-uniform thermal structure (Hu et al., 2017). This non-zero ATAG not only reflects the spatial variability of the baroclinic structure but also provides the thermodynamic background favorable for large-scale anomalous ascending and descending motions, thereby contributing to the generation and maintenance of meridional and zonal vertical circulations through dynamic-thermodynamic coupling. Thermodynamic processes such as diabatic heating and air-sea interactions thus serve as important sources for these temperature gradient anomalies. Moreover, recent non-uniform global warming, through its modification of regional temperature gradients, may further modulate the long-term *evolution of these vertical circulations (Hu et al., 2018a, b). This physical interpretation is consistent with the quasi-geostrophic omega equation framework, in which the Laplacian of temperature advection, essentially a manifestation of the horizontal temperature gradient and its spatial structure, constitutes one of the primary forcing terms for large-scale vertical motion in the extratropics.*

3, The authors argue that several patterns correspond to known modes like the Silk Road Pattern (SRP), British–Baikal Corridor (BBC), and circumglobal teleconnection (CGT). I suggest to provide a summary table or schematic that explicitly maps the new 3D patterns to previously known teleconnections (SRP, CGT, BBC, BOC, Summer NAO) with key references. This will help readers quickly understand the hierarchy and novelty of your findings.

Response:

We thank the reviewer for this suggestion. Following the recommendation, we have added a comprehensive summary table (new Table 1) in Section 3.1, which lists for each of the 14 patterns its abbreviation, full name, underlying stream function, endpoint coordinates, and the closest previously documented teleconnection counterpart with key references. This table allows readers to quickly identify the correspondence between our 3D patterns and known modes such as SRP, CGT, BBC, BOC, and the summer NAO, and to understand the hierarchy and novelty of our findings.

Table 1. Geographic names, endpoint coordinates, endpoint correlations, and analogous known patterns for the 14 vertical circulation teleconnections identified in this study.

Abbreviation	Full name	Pole A (lon, lat)	Pole B (lon, lat)	Correlation	Similar known pattern
HP	Polar I	(87.5°E, 87.5°N)	(95°W, 87.5°N)	-0.89	
HCB	Canadian-Bermuda	(100°W, 50°N)	(67.5°W, 42.5°N)	-0.76	ANA (0.69)
HCST	Caspian Sea-Tarim	(50°E, 45°N)	(82.5°E, 40°N)	-0.73	SRP (0.89)
HSK	Central Siberia-Kara Sea	(127.5°E, 60°N)	(75°E, 80°N)	-0.71	BBC (-0.77)
HGS	Greenland-Scandinavia	(40°W, 67.5°N)	(7.5°E, 62.5°N)	-0.68	
HBA	Black Sea-Aleutian	(30°E, 40°N)	(162.5°W, 57.5°N)	-0.68	
HUB	Ural-Baltic	(17.5°E, 52.5°N)	(57.5°E, 62.5°N)	-0.67	BOC (0.74)
WP	Polar II	(12.5°W, 87.5°N)	(167.5°E, 87.5°N)	-0.90	
WMCS	Mongolia-Central Siberia	(107.5°E, 42.5°N)	(100°E, 67.5°N)	-0.77	
WWSJ	West Siberian-Junggar	(77.5°E, 65°N)	(87.5°E, 45°N)	-0.74	
WGA	Greenland Sea-Azores	(5°W, 70°N)	(20°W, 45°N)	-0.76	SNAO (-0.67)
WOM	Ogasawara-Mexico	(155°E, 25°N)	(95°W, 25°N)	-0.75	
WCV	Chukchi Sea-Victoria	(172.5°W,80°N)	(102.5°W, 70°N)	-0.72	
WBA	Bering Strait-Aleutian	(162.5°W, 70°N)	(155°W, 50°N)	-0.70	

Note: SRP, BBC, BOC, and SNAO denote the Silk Road Pattern, British-Baikal Corridor, British-Okhotsk Corridor, and summer North Atlantic Oscillation, respectively. References: SRP (Enomoto et al., 2003; Lu et al., 2002); BBC and BOC (Xu et al., 2019b, 2022); SNAO (Greatbatch and Rong, 2006).

4, Does the 3D perspective reveal previously underappreciated vertical structures for these known patterns? Or are these entirely new modes? If the latter, the manuscript should argue why these significant modes were missed by traditional 2D frameworks.

Response:

We thank the reviewer for this important question. Our answer is that the 14 patterns represent a combination of both. As summarized in Table 1, several of the identified patterns, including HCST, HSK, HUB, and WGA, exhibit horizontal structures that closely correspond to well-established teleconnections such as the Silk Road Pattern (SRP), the British–Baikal Corridor (BBC), the British–Okhotsk Corridor (BOC), and the summer North Atlantic Oscillation (SNAO). For these patterns, our three-dimensional framework provides a possible dynamical interpretation by revealing the coupled vertical circulation cells that underlie their horizontal expressions. These vertical circulation cells have always existed in the real atmosphere, yet they have remained diagnostically invisible in traditional two-dimensional analyses.

At the same time, some of the identified patterns, such as WCV and WMCS, do not have obvious counterparts in the existing literature. We consider these as potentially new modes of low-frequency variability. For instance, the horizontal circulation pattern associated with WCV bears a close resemblance to observed summer circulation anomalies during certain extreme years (e.g., 2018; Figure R1), and WMCS shows a similar correspondence with the 2015 summer circulation anomalies (Figure R2). These similarities suggest that these patterns may capture real, albeit less frequent, modes of variability. The fact that these patterns have not been documented in previous studies does not diminish their physical significance; rather, it reflects the methodological limitations of traditional two-dimensional frameworks.

Why, then, have these vertical structures—whether the newly revealed counterparts of known teleconnections or the potentially new modes—not been adequately recognized previously? This question may be related to the methodological foundations of traditional teleconnection analyses. Conventional approaches, such as empirical orthogonal function (EOF) analysis, regression analysis, or single-point correlation methods applied to geopotential height or stream function of horizontal fields, are primarily concerned with the spatial covariance structures of horizontal circulation and their dominant modes of variability. These methods tend to identify horizontal anomaly centers and their wave train propagation pathways, but they generally do not focus on resolving the vertical structure of the circulation. Vertical motion, particularly the mid-latitude omega field, is typically provided as a diagnostic variable in reanalysis datasets, yet it has rarely been used as a primary variable for identifying and characterizing teleconnection patterns in traditional analyses. Consequently, the vertical circulation structures accompanying horizontal teleconnection wave trains may not have been fully revealed within conventional two-dimensional frameworks. In contrast, the 3P-DGAC framework employed in this study is capable of explicitly decomposing the three-dimensional atmospheric circulation into horizontal, meridional, and zonal vertical components (Hu et al., 2017, 2018a, b), thereby providing a new avenue for the systematic identification and direct analysis of vertical circulation structures. This methodological feature may help to reveal the vertical counterparts of known horizontal teleconnections and to further identify potential new modes that have received insufficient attention within traditional two-dimensional frameworks.

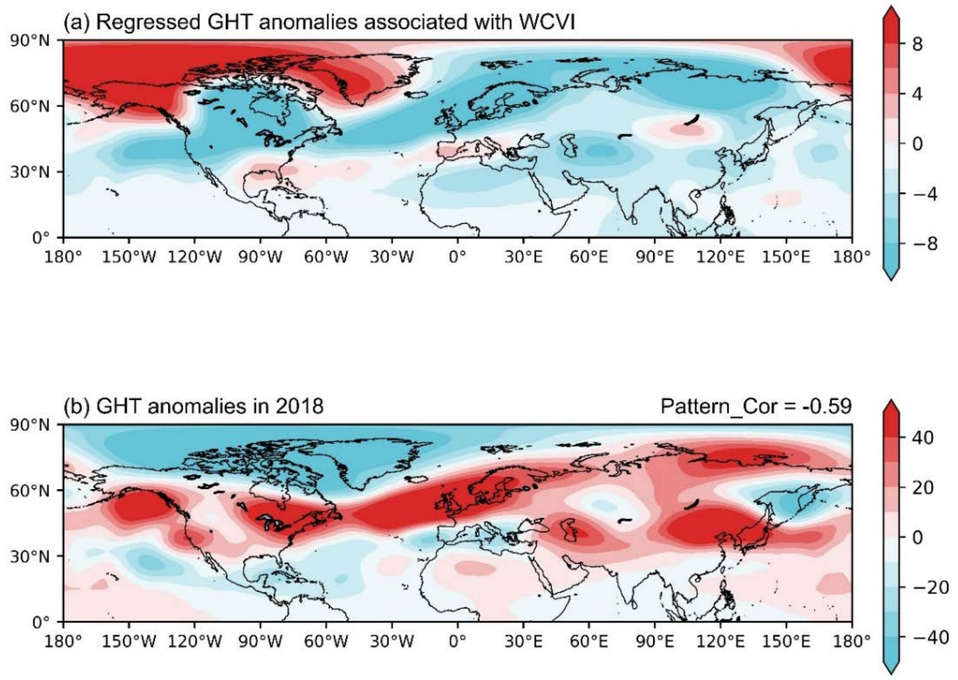

Figure R1. Regressed horizontal circulation mode of WCV and the 2018 summer circulation anomaly. (a) Regressed summer 200-hPa geopotential height anomalies associated with the WCV index for the period 1979–2022. (b) Observed summer 200-hPa geopotential height anomalies in 2018. The spatial correlation coefficient between the two fields is shown in the panel.

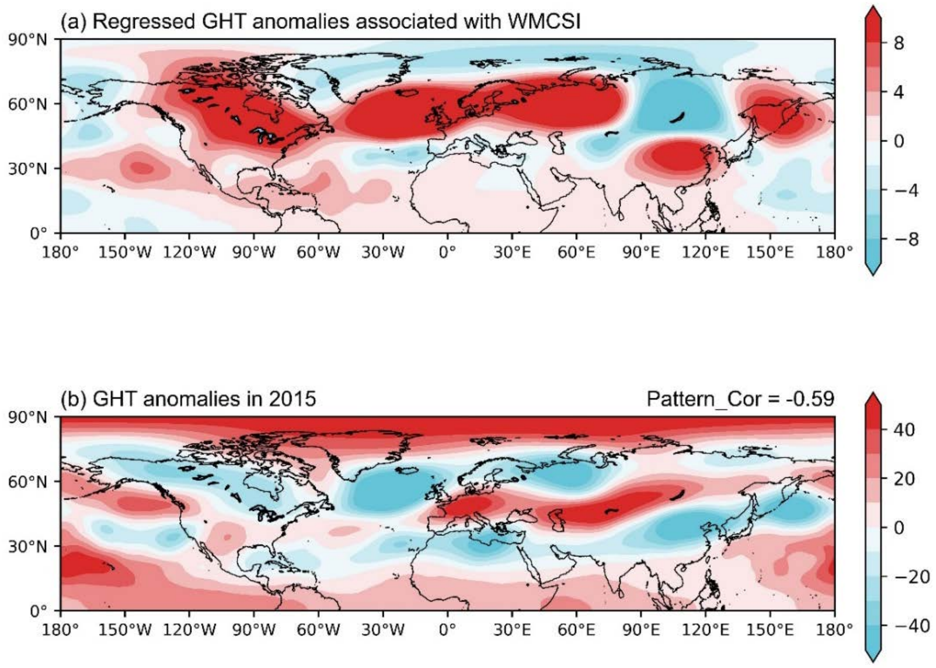

Figure R2. As in Figure S10, but for WMCS and the 2015 summer circulation anomaly. (a) Regressed summer 200-hPa geopotential height anomalies associated with the WMCS index for the period 1979–2022. (b) Observed summer 200-hPa geopotential height anomalies in 2015. The spatial correlation coefficient between the two fields is shown in the panel.

Thank you for this thoughtful question. Some of these points are briefly foreshadowed in the Introduction, particularly the limitations of conventional two-dimensional approaches; we have now expanded and clarified them in the revised Discussion to make the distinction between known counterparts and potentially new modes more explicit.

5, Could you provide the explained variance for each of the 14 teleconnection patterns? It is crucial to know which patterns are the most dominant and statistically significant to assess their relative importance in the climate system.

Response:

We thank the reviewer for this important question and for the opportunity to clarify this point. We agree that the original manuscript did not explain this issue as clearly as it should have. In the revised manuscript, we have clarified in Discussion why our reconstruction framework does not produce a single explained-variance value for each of the 14 patterns.

We would like to explain why a single explained-variance value for each pattern is not available in our reconstruction framework, and why we consider such a value to be of limited applicability for this particular framework.

Our reconstruction strategies for SAT and circulation fields differ fundamentally, and neither approach lends itself to a simple variance decomposition.

For the SAT reconstruction, we use a grid-point-by-grid-point stepwise regression with the 14 indices as candidate predictors. At each grid point, the selected predictors differ, so the regression equation is spatially variable. A teleconnection pattern typically affects a limited and regionally distinct spatial domain. Therefore, a single global explained-variance value would not reflect the spatially varying contribution of each pattern. A pattern that explains only a small fraction of the hemispheric mean variance may still be important for regional temperature anomalies. For this reason, we do not report a single explained-variance value for each pattern.

For the circulation reconstruction, the logic is even less compatible with a variance decomposition. We do not perform grid-point regression. Instead, for each target year, we identify the one to three indices with the largest deviations from their climatological means and reconstruct the circulation field by directly superimposing the horizontal patterns associated with these dominant indices. This year-specific strategy preserves the spatial integrity of each pattern. The reconstruction skill in a given year depends mainly on the most active pattern or patterns in that year, for example WWSJ in 2022 (Fig. 8 in the revised manuscript; Fig. R3 in this response letter). Because the reconstruction is not based on a single regression model over all grid points, the explained variance of individual patterns is not well defined.

We have revised the corresponding text in the Discussion (Lines 432–436) to make this rationale clearer.

Lines 432–436

It should also be noted that this framework does not provide a single explained-variance value for each of the 14 patterns, because the SAT reconstruction is grid-point-specific while the circulation reconstruction is year-specific. The relative importance of individual patterns is therefore assessed through their regional contributions and their activity in individual years rather than through a single global variance metric.

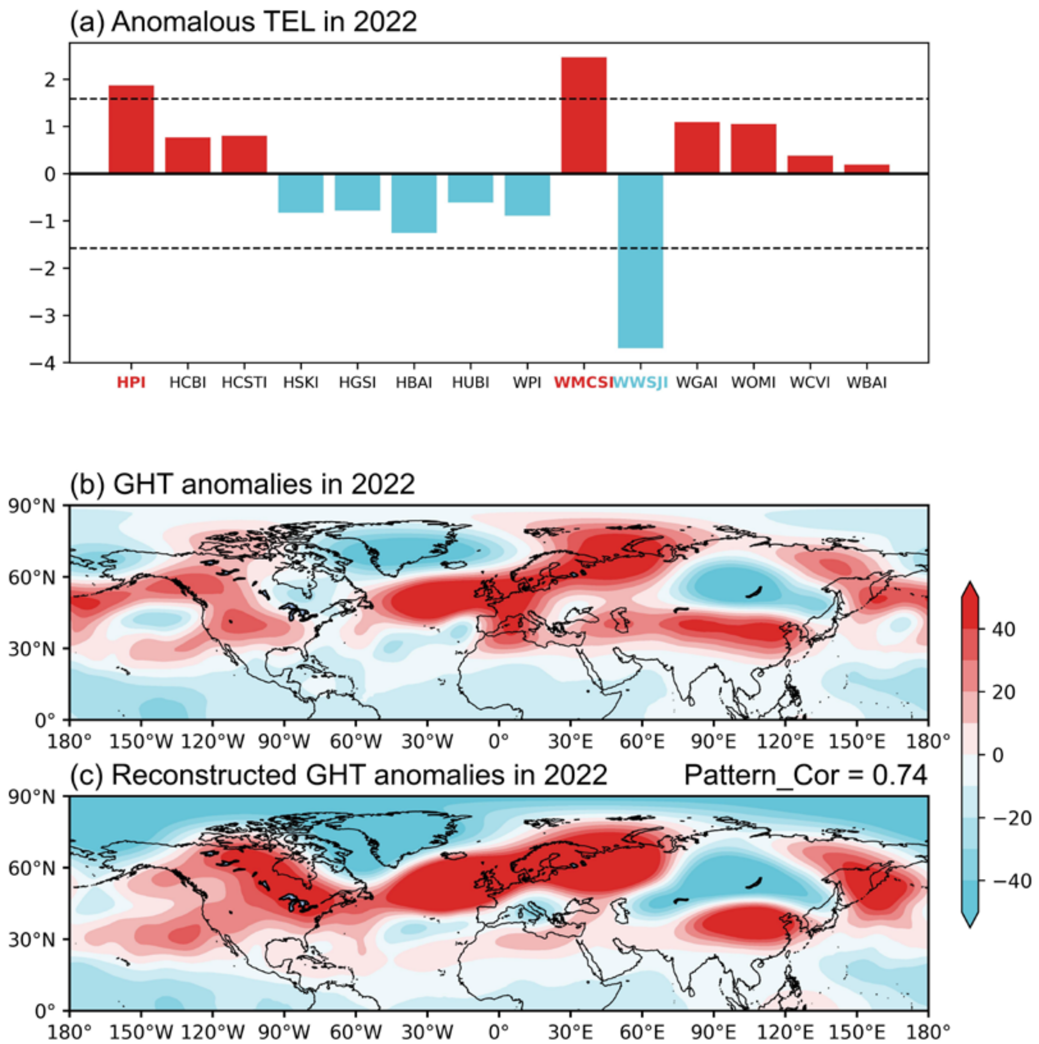

Figure R3. Reconstructed circulation anomalies in 2022. (a) Indices of teleconnection patterns in 2022. The dashed lines denote the reference line of the ± 1 standard deviation. (b) Summer GHT anomalies (shading, units: gpm) in the NH during the summer of 2022. (c) Reconstructed summer GHT anomalies (shading, units: gpm) in the NH during the summer of 2022.